

# Detection of Curved Road Edges in Radar Images Via Deformable Templates

Bing Ma\*

Sridhar Lakshmanan<sup>†</sup>

Alfred O. Hero\*

## Abstract

Three methods of detecting road edges in millimeter-wave radar images are presented in this paper. All of them are based on deformable template priors and random field likelihoods. The first method is formulated in a Bayesian setting and employs an adaptive MAP estimate. The second method is a modification of the first, using a novel weighting scheme. The third method is based on a three-region indicator matrix which is used to impose the non-linear constraints implicit on road geometry via addition of a sum of quasi-quadratic matrix forms to the log-normal likelihood. Unlike the first two methods, that employ the Metropolis algorithm to find the optimal road edges, the third method uses a deterministic recursive scheme designed to find the optimal indicator matrix. Experimental results are presented to show the advantages of these methods.

## 1 Introduction

In this paper, we deal with the problem of locating curved and parallel road edges in radar data that are acquired from an imaging platform mounted on a stationary automobile. The goal of road detection algorithms is to find the road edges without an existing model of road geometry, and do so in situations where there may be a great deal of clutter in the images due to cars on the road, complicated backscatter from off-road structures, etc.

Many prior detection algorithms that are applicable for structured edges such as road boundaries are edge-based and threshold the image gradient magnitude to detect edges. The performance of these edge detection algorithms is good when the images have uniform regions with good separation between the regions. However, in real road scenes it is difficult to select a threshold which eliminates noise edges without also eliminating many of the road points of interest. This problem is particularly severe in C band, L band or X band radar images (see Fig.1(b) and Fig.2(b)), which have both a lot of texture

and low contrast<sup>1</sup>. Therefore, the conventional edge detection algorithms are not suitable for our problem.

In order to overcome this difficulty, we make use of deformable template approaches which do not require thresholding the image gradient magnitudes. This allows weak edge points which are consistent with a prior geometric model of possible road boundary shapes to overrule strong edge points which are not consistent with the prior geometric model.

In this paper, we will present three different methods for this edge detection problem. All of them are based on deformable template priors[1] and random field likelihoods similar to [2].

## 2 Detection Algorithms

In all the three methods, the road edges in the radar image are extracted by identifying “homogeneous” regions in the image. The road boundaries separate the image into three uniform regions which associate with the road surface, the left side of the road, and the right side of the road.

Let  $\mathcal{L} = \{(x, y), 0 \leq x \leq x_{max}, 0 \leq y \leq y_{max}\}$  denote the Cartesian coordinates of the pixels of the millimeter-wave image  $Z$ . The radar imaging likelihood is described using the conditional probability that the random field  $Z$  takes on a realization  $z$  (corresponding to the radar observation), given that the road edge information is known,

$$P(Z = z \mid \text{road geometry}) = \prod_{(x,y) \in \mathcal{L}} \frac{1}{z_{xy} \sqrt{2\pi\sigma_{xy}^2}} \exp\left\{-\frac{1}{2\sigma_{xy}^2}(\log z_{xy} - \mu_{xy})^2\right\} \quad (1)$$

where  $\mu_{xy}, \sigma_{xy}^2$  denote the mean and variance of the region where the pixel  $(x, y)$  lies. Obviously, this imaging likelihood is log-normal distributed[3].

### 2.1 Method 1. Adaptive Log-normal Method

In almost all cases, we can assume that *a priori* knowledge regarding the shape of the road edges in an image

<sup>1</sup>In a typical millimeter-wave radar image, near-range power values exhibit a considerable amount of contrast and textural variability, whereas far range power values exhibit neither a considerable amount of contrast nor textural variability.

\*Bing Ma and Alfred O. Hero are with the Department of Electrical Engineering and Computer Science, The University of Michigan — Ann Arbor, MI 48109.

<sup>†</sup>Sridhar Lakshmanan is with the Department of Electrical and Computer Engineering, The University of Michigan — Dearborn, MI 48128.

is available. A common shape model used in road edge detection algorithms assumes that road boundaries can be approximated by concentric arcs on a flat ground plane. Such arcs, at least within a reasonable field of view, are well approximated by parabolic curves. In method 1, the road boundaries are parameterized as two parallel and parabolic curves in the form

$$x = \frac{1}{2}ky^2 + my + b_L(b_R) \quad (2)$$

where parameter  $k$  is the curvature of the arc,  $m$  is the tangential orientation and  $b_L(b_R)$  is the offset corresponding to the left(right) road edge. The two road boundaries share the same parameters  $k$  and  $m$ . We assume the parameters are uniformly distributed over the space  $R^4$ .

The physical characteristics of the radar imaging process is described by the log-normal random field model which is represented by Eqn.(1). Thus, the road edges detection problem is posed in a Bayesian framework where the deformable template plays the role of a prior and the log-normal pdf plays the one of a likelihood. The Maximum *A Posteriori*(MAP) estimator is used to find the optimal deformation parameter values:

$$\begin{aligned} & (k^*, m^*, b_L^*, b_R^*) \\ &= \arg \max_{(k, m, b_L, b_R)} \log P(k, m, b_L, b_R | Z = z) \\ &= \arg \max_{(k, m, b_L, b_R)} \log P(Z = z | k, m, b_L, b_R) \\ &= \arg \max_{(k, m, b_L, b_R)} \sum_{(x, y) \in \mathcal{L}} \left\{ -\log \sigma_{xy} - \frac{1}{2\sigma_{xy}^2} (\log z_{xy} - \mu_{xy})^2 \right\} \quad (3) \end{aligned}$$

Let  $(\mu^{rd}, \sigma^{rd}, N^{rd})$ ,  $(\mu^{lt}, \sigma^{lt}, N^{lt})$  and  $(\mu^{rt}, \sigma^{rt}, N^{rt})$  denote the means, standard deviations and the numbers of pixels associated with the road, left-side and right-side regions, respectively. For a given parameter set  $\{k, m, b_L, b_R\}$ , the means and standard deviations can be empirically estimated from the image data by a maximum likelihood method,

$$\begin{aligned} \mu^{rd} &= \frac{1}{N^{rd}} \sum_{(x, y) \in \mathcal{L}^{rd}} \log z_{xy} \\ (\sigma^{rd})^2 &= \frac{1}{N^{rd}} \sum_{(x, y) \in \mathcal{L}^{rd}} (\log z_{xy} - \mu^{rd})^2 \quad (4) \end{aligned}$$

where  $\mathcal{L}^{rd} = \{(x, y), (x, y) \in \mathcal{L}, x \geq \frac{1}{2}ky^2 + my + b_L, x \leq \frac{1}{2}ky^2 + my + b_R\}$ . Similarly  $\mu^{lt}$  &  $\sigma^{lt}$ ,  $\mu^{rt}$  &  $\sigma^{rt}$  can be obtained by (i)replacing  $N^{rd}$  in Eqn.(4) with  $N^{lt}$  and  $N^{rt}$ , and (ii) replacing  $\mathcal{L}^{rd}$  in Eqn.(4) with  $\mathcal{L}^{lt} = \{(x, y), (x, y) \in \mathcal{L}, x < \frac{1}{2}ky^2 + my + b_L\}$  and  $\mathcal{L}^{rt} = \{(x, y), (x, y) \in \mathcal{L}, x > \frac{1}{2}ky^2 + my + b_R\}$ .

The log-normal likelihood in Eqn.(3) is modified by re-substituting these estimated parameters back in, thereby making the method adaptive,

$$\begin{aligned} & (k^*, m^*, b_L^*, b_R^*) \\ &= \arg \max_{(k, m, b_L, b_R)} (-N^{rd} \log \sigma^{rd} - N^{lt} \log \sigma^{lt} - N^{rt} \log \sigma^{rt}) \quad (5) \end{aligned}$$

The objective function in Eqn.(5) is non-concave with many local maxima, hence we employ the Metropolis algorithm[4] with a geometric annealing schedule[5] to perform this maximization,

1. Set  $i = 0$ , and initialize  $\{k^{(0)}, m^{(0)}, b_L^{(0)}, b_R^{(0)}\}$ .
2. Calculate  $L^{(i)} = \log P(k^{(i)}, m^{(i)}, b_L^{(i)}, b_R^{(i)} | Z = z)$ .
3. Pick  $\{\tilde{k}, \tilde{m}, \tilde{b}_L, \tilde{b}_R\}$  at random among all the possible parameter values in the neighborhood of  $\{k^{(i)}, m^{(i)}, b_L^{(i)}, b_R^{(i)}\}$ .
4. Calculate  $\tilde{L} = \log P(\tilde{k}, \tilde{m}, \tilde{b}_L, \tilde{b}_R | Z = z)$ .
5. Calculate  $\rho^{(i)} = \exp\left(\frac{\tilde{L} - L^{(i)}}{T^{(i)}}\right)$ ,  
where  $T^{(i)} = T_{init} \left(\frac{T_{final}}{T_{init}}\right)^{\left(\frac{i+1}{\text{max iter}}\right)}$ .
6. Update  $\{k^{(i+1)}, m^{(i+1)}, b_L^{(i+1)}, b_R^{(i+1)}\}$   

$$= \begin{cases} \{\tilde{k}, \tilde{m}, \tilde{b}_L, \tilde{b}_R\} & \text{if } \rho^{(i)} \geq 1 \\ \{\tilde{k}, \tilde{m}, \tilde{b}_L, \tilde{b}_R\} & \text{w.p. } \rho^{(i)} \text{ if } \rho^{(i)} < 1 \\ \{k^{(i)}, m^{(i)}, b_L^{(i)}, b_R^{(i)}\} & \text{otherwise} \end{cases}$$
7. Set  $i = i+1$  and go to step 2.

## 2.2 Method 2. Weighted Log-normal Method

From Eqn.(5) we can see that our objective is trying to minimize  $N^{rd} \log \sigma^{rd} + N^{lt} \log \sigma^{lt} + N^{rt} \log \sigma^{rt}$ , i.e., trying to minimize the variances of the three regions. However, in the radar images, it is clear that the backscatter distribution of the road is virtually homogeneous while the backscatter distributions of the roadsides are much more complicated. Therefore, we might prefer having an even smaller variance in the road region at the price of having slightly larger variances in the roadside regions.

In method 1, the variances are weighted proportionately to the number of pixels in their respective regions. In order for  $\sigma^{rd}$  to weigh more heavily, in terms of its contribution to the likelihood,  $N^{rd}$  would have to proportionately large. The same is true for the other two regions as well. This characteristic is illustrated in Fig.2(c), where one can see that the road edges detected by Method 1 yields a 3-region estimate in which the road is wider than necessary (actual). Also, the edges detected by method 1 are unduly influenced by bright point scatterers, particularly in far ranges where the contrast (difference) between the road and roadside regions is minimal. In fact one can see in Fig.2(c) that method 1 is prone to giving wrong curvature estimates (it estimates the road as curving right, while in reality the road is curving left).

In order to re-enforce our *a priori* belief that road pixels tend to be homogeneous (at least compared to the pixels belonging to either side of the road), and to overcome the undue influence of bright point scatterers, we propose a new method that gives the region of the road a different weight  $w^{rd}$  ( $0 < w^{rd} < 1$ ) from those given to the roadside regions. The weighted log-normal method, when coupled

with a penalty function  $\alpha(\cdot)$ ,<sup>2</sup> yields considerably better results as shown in Fig.2(d).

$$\begin{aligned} & (k^*, m^*, b_L^*, b_R^*) \\ = & \arg \max_{(k, m, b_L, b_R)} (-N^{lt} \log \sigma^{lt} - N^{rt} \log \sigma^{rt} \\ & - w^{rd} N^{rd} \log \sigma^{rd} + \log \alpha(k, m, b_L, b_R)) \end{aligned} \quad (6)$$

where

$$\alpha(k, m, b_L, b_R) = \frac{2}{\pi} \text{atan}(d_{width} \times (b_R - b_L)) \quad (7)$$

### 2.3 Method 3. Recursive Indicator Matrix Method

In both methods 1 and 2, the objective functions being optimized, with respect to the deformation parameters, are non-concave and have many local maxima. To obtain the global maxima of those objective functions, we are forced to employ stochastic algorithms such as Metropolis. While these algorithms are simple to devise and program, they have to be carefully tuned before they can be employed over a large class of images. To remedy this problem, a new three-region indicator matrix based formulation is presented. The geometric constraints of the road edges imposed by the deformable template are rewritten in terms of constraints on the indicator matrix  $I_i$ .  $I_i$  is a  $mn \times 3$  matrix (the dimension of the radar image is  $m \times n$ ) and its  $p$ -th row  $[c_{p1}, c_{p2}, c_{p3}]$  ( $0 \leq p \leq mn - 1$ ) corresponds to a pixel in the radar image. Let  $j = 1, 2, 3$  denote the left-side, road and right-side region, respectively. If pixel  $p$  is in the  $j$ -th region, then

$$c_{pk} = \begin{cases} 1 & \text{if } k = j \\ 0 & \text{otherwise} \end{cases} \quad (8)$$

With this indicator matrix Eqn.(3) can be reformulated as

$$I_i^* = \arg \min_{I_i} \| (I - I_i(I_i^T I_i)^{-1} I_i^T) \log Z \|^2 \quad (9)$$

The generic portion of the constraint expressed via Eqn.(2), namely, that the road edges be smooth and connected, can also be expressed in terms of the indicator matrix  $I_i$ :

$$\min_{I_i} \| I_i - \text{shift}(I_i) \|^2 \quad (10)$$

Combining Eqns.(9) and (10), we can recast an alternative deformable template minimization problem in terms of the indicator matrix  $I_i$ :

$$\begin{aligned} I_i^* = \arg \min_{I_i} \{ & \| (I - I_i(I_i^T I_i)^{-1} I_i^T) \log Z \|^2 \\ & + \| I_i - \text{shift}(I_i) \|^2 \} \end{aligned} \quad (11)$$

<sup>2</sup>This penalty function is to prevent the detected road from being too narrow. Without the  $\alpha(\cdot)$  term, maximization of the weighted likelihood in Eqn.(6) tends to yield estimates where the left and right road edges collapse to be the same.

As it stands, the objective function in Eqn.(11) is not convex w.r.t.  $I_i$ , and hence difficult to minimize. However, we can design a recursive scheme to simplify the optimization,

$$\begin{aligned} I_i^{(k)*} = \arg \min_{I_i^{(k)}} \{ & \| (I - I_i^{(k)}(I_i^{(k-1)T} I_i^{(k-1)})^{-1} I_i^{(k)T}) \log Z \|^2 \\ & + \| I_i^{(k)} - \text{shift}(I_i^{(k)}) \|^2 \} \end{aligned} \quad (12)$$

which is a quadratic integer optimization problem.

## 3 Experimental Results

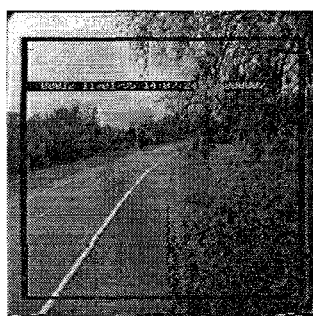
We have applied the three deformable template methods described in the previous sections to locate curved road edges in actual ground-level millimeter-wave radar images<sup>3</sup>. Shown in Figs.1(b) and (a) are an original radar image and accompanying visual image (the goal of also displaying visual images is just to give readers a clearer image of the ground truth, in our work, however, we only make use of radar images to detect road edges); the results obtained by applying Methods 1, 2 and 3 are shown in Figs.1(c), (d) and (e), respectively. As one can see, all the three methods give comparable results, and indeed those results are very close to the ground truth. In addition, to illustrate the improvement of Method 2 over Method 1, we consider another visual/radar image pair in Figs.2(a) and (b). For this case, the result of detecting the road boundaries using method 1 is shown in Fig.2(c) and the result using method 2 is shown in Fig.2(d).

## 4 Concluding Remarks

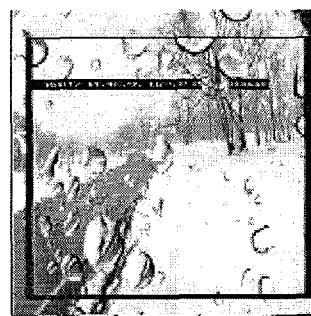
In this paper we developed three different methods for detecting road edges in radar images. All of them are based on deformable template priors, random field likelihoods, and Bayesian estimation. The first method is an adaptive MAP estimate method, the second method is a modified version of the first via a novel weighting strategy and the addition of a penalty term. The third method relies on an indicator matrix (re)formulation of the problem — specifically, the rigid geometric constraints imposed by the deformable template prior are replaced by some quadratic constraints on the indicator matrix and the original objective function is recast in such a way that it is recursively convex w.r.t. the indicator matrix. The net result is that method 3 uses a deterministic iterative algorithm for finding the optimal road boundaries, as opposed to the stochastic (Metropolis) algorithms used in Methods 1 and 2.

Since none of the three methods makes use of the noise-sensitive gradient magnitude of the radar images, they

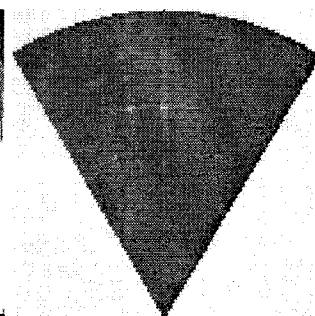
<sup>3</sup>These images were all obtained from a sensor platform mounted on top of WOLVERINE I (a self-contained test-bed HMMWV). The platform contains a 77GHz FMCW radar sensor which has range and azimuthal resolution of 0.5m and 1°, respectively. The radar's range extends out to 128m and spans a 64° horizontal field-of-view.



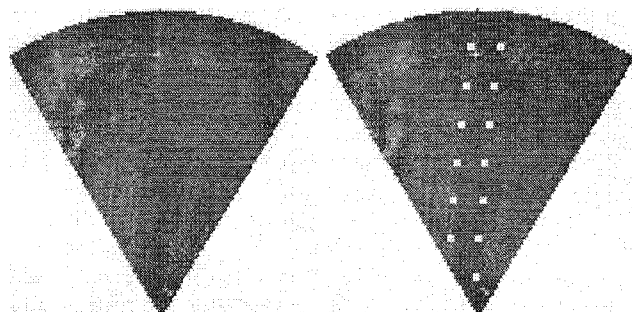
(a)



(a)

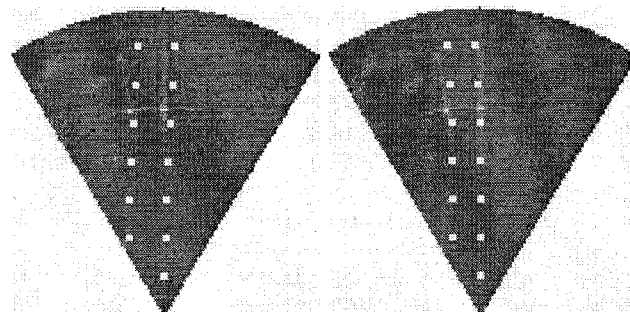


(b)



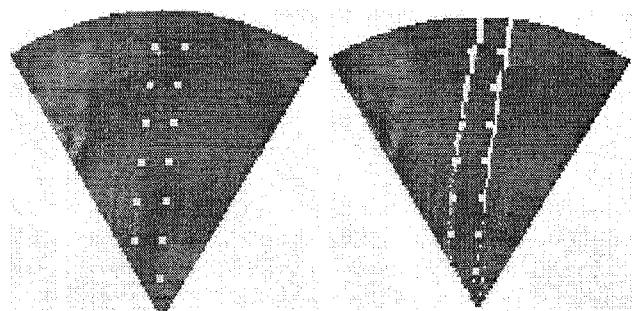
(b)

(c)



(c)

(d)



(d)

(e)

Figure 1: (a) Visual image, (b) Radar image, (c) Result from Method 1, (d) Result from Method 2, and (e) Result from Method 3

overcome the shortcomings of the edge-based detection algorithms. The results show that the methods we present in this paper promise to be better than the edge-based detection algorithms, particularly, when the edge gradient has an unusually small SNR, or when the roadsides contain bright point scatterers.

Figure 2: (a) Visual image, (b) Radar image, (c) Result from Method 1, and (d) Result from Method 2

## References

- [1] Y. Amit, U. Grenander and M. Piccioni, "Structural image restoration through deformable templates," *J. Am. Statist. Assoc.*, Vol. 86, pp.376-387, 1991.
- [2] S. Lakshmanan and D. Grimmer, "A Deformable Template approach to detecting Straight Edges in Radar Images," *IEEE Trans. Pattern Anal. Mach. Intell.*, Vol. 18, pp. 438-443, 1996.
- [3] J. Aitchison and J. A. C. Brown, *The Log-normal Distribution*, Cambridge University Press, 1957.
- [4] K. C. Kluge and S. Lakshmanan, "A Deformable-Template Approach to Lane Detection," *Proc. Intell. Vehic. '95 Symp.*, Sept., 1995.
- [5] D. N. Strenki and S. Kirkpatrick, "Analysis of Finite-length Annealing Schedules," *Algorithmica*, 6: pp. 346-366, 1991.